# Transmission electron microscopy of weakly deformed alkali halide crystals

H. Strunk

Classification
*Physics Abstracts*
7.166 — 7.222

# TRANSMISSION ELECTRON MICROSCOPY OF WEAKLY DEFORMED ALKALI HALIDE CRYSTALS

H. STRUNK

Max-Planck-Institut für Metallforschung, Institut für Physik, Büsnauer Strasse 171, 7000 Stuttgart 80, Germany

(*Reçu le 1er octobre 1976, accepté le 10 décembre 1976*)

**Résumé.** — La microscopie électronique par transmission (TEM) est appliquée à l'étude de l'arrangement des dislocations dans des cristaux d'halogénures alcalins orientés suivant l'axe [001] (orientation pour glissement quadruple) déformés jusqu'au stade I de la courbe d'écrouissage. L'étude a porté principalement sur des cristaux de NaCl à (0,1-1) mole % de NaBr, car ils présentent un stade I particulièrement long. Le temps disponible pour l'observation des spécimens est limité par des lésions d'irradiation dans le microscope. Une réduction optimale du taux de production de ces lésions est obtenue par une combinaison de techniques expérimentales brièvement décrites.

Les cristaux se déforment essentiellement par glissement simple. D'après les observations, la déformation au stade I de cristaux de NaCl purs ou faiblement alliés est caractérisée par le glissement des dislocations vis qui se courbent entre les sauts et traînent derrière elles des dipôles de dislocations. Dans les cristaux à plus de 0,5 mole % de NaBr, ce phénomène n'est plus observé. Ceci est attribué à l'importance croissante du durcissement de la solution solide.

**Abstract.** — Transmission electron microscopy (TEM) is applied to the investigation of the dislocation arrangement of [001]-orientated alkali halide crystals (orientation four quadruple slip) deformed into stage I of the work-hardenig curve. The investigations pertain mainly to NaCl-(0.1-1) mole-% NaBr crystals, because these exhibit a relatively long stage I. The time available for observing the specimens is limited by the ionization radiation damage occuring in the microscope. An optimum reduction of the damage rate is achieved by a combination of several experimental techniques that are briefly outlined.

The crystals deform essentially in single glide. According to the observations, stage I deformation of pure and weakly alloyed NaCl crystals is characterized by the glide of screw dislocations, which bow out between jogs and drag dislocation dipoles behind them. In crystals with $\gtrsim$ 0.5 mole-% NaBr this process is not observed to occur. This is attributed to the increased importance of solid solution hardening.

1. **Introduction.** — It is only some years ago that transmission electron microscopy (TEM) was first applied successfully to the investigation of the dislocation arrangement in plastically deformed pure NaCl crystals (e.g. [1, 2]). Since that time instructive insight into the deformation mechanisms has been obtained. This is especially true for stage II work-hardening, in which a moderate dislocation density is present convenient for an analysis by TEM [1-3]. In general, NaCl crystals deform essentially in macroscopic single glide on one $\{\,\bar{1}01\,\}\langle\,101\,\rangle$-system (primary glide system), although at least two (in [001]- and [110]-orientated crystals four) systems of this type have the same largest Schmid factor. Stage II is characterized by the onset of short-range secondary glide and the interaction of the primary with the secondary dislocations [3, 4].

The present paper reports on an investigation of deformation mechanisms typical of stage I of [001]-orientated crystals. In pure crystals stage I is short and the acquired dislocation density is much too low for a satisfactory TEM investigation. Hence NaCl crystals with a content of up to 1 mole-% NaBr which exhibit a longer stage I have been used. By alloying with monovalent dopants strong electrostatic interactions between dopant and dislocations are avoided; divalent dopants alter the dislocation behaviour severely (e.g. [5, 6]). The conclusions drawn from the set of differently doped crystals used permits both an extrapolation to pure NaCl and a distinction of alloy-induced changes in the glide properties.

2. **Glide elements and experimental techniques.** — 2.1 NOTATION OF GLIDE ELEMENTS. — The chosen

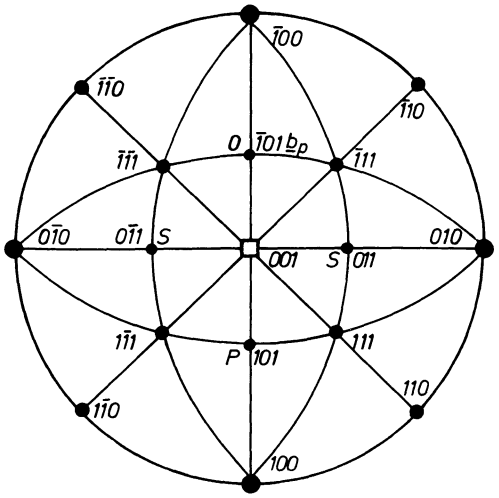


FIG. 1. — Stereographic projection and glide elements of [001]-orientated crystals. P : primary glide plane, $\mathbf{b}_p$ : primary Burgers vector, O : orthogonal glide plane, S : oblique glide plane.

notation is shown in figure 1 and agrees with that one used earlier [4]. In the following the term secondary dislocations comprises all dislocations having other than primary Burgers vector. The densities of the dislocations with Burgers vector of the primary and secondary glide planes are denoted by $\rho_{\text{prim}}$ and $\rho_{\text{sec}}$ respectively. The latter is, where appropriate, subdivided into $\rho_{\text{orth}}$ and $\rho_{\text{sec e.o.}}$, where the first refers to the orthogonal dislocations and the second to all other secondary (*secondary excluding orthogonal*) dislocations.

2.2 CRYSTAL PREPARATION AND DEFORMATION. — Cylindrical crystals ~ 4 cm in diameter and ~ 6 cm in height, grown by Korth, Kiel, from NaCl and NaBr (quality p.a.) in the compositions NaCl-0.1, 0,5 and 1.0 mole-% NaBr, were cleaved to small pieces, which were carefully polished on a wetted cloth to the final dimensions of 4 × 4 × 18 mm$^3$. In order to remove cleavage strains and to reduce the initial dislocation density, these crystals were annealed in air at about 750 °C for at least 24 hours, and subsequently slowly cooled down ($\leqslant$ 50°/h.). Compressional deformation was performed at room temperature in an Instron machine at an initial strain rate of $\dot{\varepsilon} = 3.7 \times 10^{-4}\ \text{s}^{-1}$ to a resolved strain of $\varepsilon = 6.9\ \%$.

2.3 TRANSMISSION ELECTRON MICROSCOPY. — The essential prerequisite for TEM of alkali halides in a routine-like fashion is the reduction of the severe radiation damage occurring in these crystals under normal circumstances due to electronic excitations produced by the incident electrons. The radiationless decay of the generated excited states leads to the production of interstitial defects in the anion sublattice by a collision sequence [7]. These defects agglomerate rapidly to visible clusters, the contrasts of which mask the contrasts of the dislocations introduced by plastic deformation. The different experimental possibilities offered to reduce the damage rate during observation, as outlined in [3], have been combined in the present investigation to optimize the available observation time.

i) The excitation rate is minimized by applying an extremely low beam current density (about $10^{-3}$ A/cm$^2$) and a high accelerating voltage (400 kV) [1], at which the ionization cross-section is approximately minimized. The use of highly sensitive photo-plates is imperative (Agfa Curix P RP).

ii) The specimens are observed at low temperature ($\lesssim$ 20 K). This permitted relatively early the study of irradiation damage in alkali halides [8]. At low temperature the thermal diffusion of the generated defects is impeded and the conversion of excited states into the interstitial defects is essentially replaced by a luminescent decay [7].

iii) Further, at the low temperatures applied, the $Br^-$ content causes an increase in lifetime compared to pure NaCl by a factor of approximately 10 (depending on the concentration). The $Br^-$-ion is 7 % larger than the substituted $Cl^-$-ion ; one explanation for the delayed agglomeration may be that the collision sequences in the anion sublattice may be stopped at the $Br^-$-ions. Thus, at the $Br^-$-densities used, the interstitial comes to rest at a distance from its vacancy within the spontaneous recombination volume. Delay of agglomeration is also observed for substitutional mono- and divalent cation impurities (e.g. [9]).

The preparation of electron transparent foils is outlined in [3] and shall briefly be sketched here. Slices approximately 0.8 mm thick cut from the deformed crystals are X-irradiated in order to pin the dislocations. (We used the Bremsstrahlung of a sealed-off X-ray tube (W-anode) operated at 50 kV). The dislocations would otherwise rearrange during thinning and especially during cooling in the microscope. Because of the sensitivity of the crystals to moisture the slices were thinned under waterfree conditions using methanole for prethinning and ethanole for final thinning. Electrical charging in the electron beam was prevented by evaporation of Al layers of 100 to 200 Å effective thickness onto both surfaces of the foil.

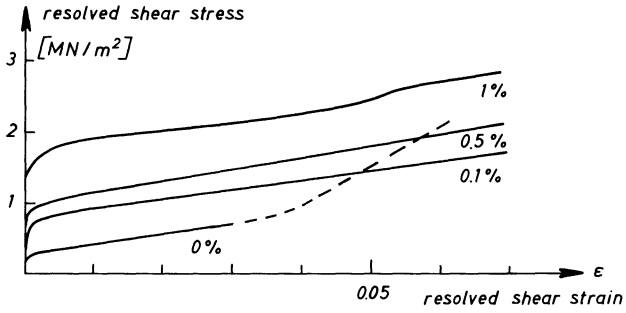


FIG. 2. — Work-hardening curves of the investigated NaCl crystals with 0, 0.1, 0.5 or 1 mole-% NaBr. The work-hardening curve of pure NaCl is extended to higher strains (dashed curve) for comparison.

3. **Experimental results.** — 3.1 WORK-HARDENING CURVES AND DISLOCATION DENSITIES. — Figure 2 shows the work-hardening curves of the crystals. The monotonic increase of the flow stress with increasing NaBr content indicates the presence of solid solution hardening. In accordance X-ray investigations of annealed NaCl-NaBr crystals [10] and our TEM yielded no evidence for phase separations. The flow stress increments $\Delta\tau$ obtained from the crystals with reference to pure NaCl crystals scattered too much to permit a decision between the $\Delta\tau \sim c^{1/2}$ and $\Delta\tau \sim c^{2/3}$ (e.g. [11]) dependences ($c$ : concentration of the solute). The observed solid solution hardening is in qualitative agreement with results of Okuda *et al.* [12]. In contrast Wimmer *et al.* [13] observed solution softening ; this is probably due to a relatively high content of divalent cation impurities (e.g. $Ca^{2+}$), as is suggested by the unusually high critical flow stress of their nominally pure crystals.

The dislocation densities observed after a deformation to $\varepsilon = 6.9$ % are plotted in figure 3*a* as a function of the NaBr content $c$. The total dislocation density $\rho_{tot}$ for pure NaCl is obtained from Hesse's etch pit data for stage I deformation [14] by extrapolation to $\varepsilon = 6.9$ %. (Our experimental data show that dislocation densities obtained by etch pit counting and by TEM can in fact be compared [15].) With reference to the pure NaCl crystals, $\rho_{tot}$ is increased in the alloy crystals by a factor of about 10 with $\rho_{prim}/\rho_{tot} = 0.6$ to 0.8 (Fig. 3*b*). For the pure NaCl crystals we expect a ratio of $\gtrsim 0.9$. With respect to the secondary dislocations, it is interesting to note that for $c \lesssim 0.5$ mole-% NaBr we found $\rho_{orth} \ll \rho_{sec\ e.o.}$, which is observed also in pure NaCl crystals [15]. Only in the case of $c = 1$ mole-% NaBr the value of $\rho_{orth}$ exceeds that of $\rho_{sec\ e.o.}$ and amounts to about 14 % of $\rho_{tot}$ (Fig. 3*b*).

3.2 TEM OF PURE NaCl. — Figure 4 shows micrographs of a thin foil cut under 35° degree to the primary glide plane of a crystal deformed by $\varepsilon = 3$ %. Because of the low dislocation density of the crystal, these micrographs are not representative for the average dislocation arrangement. They are selected to show some significant elements supporting the interpretation of our observations (e.g. section 4.2). The dominance of edge or nearly edge dislocations in dipolar and sometimes in multipolar arrangements is striking (Fig. 4*a*). The dipole widths rarely exceed 0.1 μm. Some unpaired edge dislocations can also be found.

By comparison, screw or nearly screw dislocations occur rarely, sometimes in dipole form. Also unpaired screw dislocations are observed either trailing edge dislocation dipoles or exhibiting cusps, probably due to the presence of a jog in the dislocation line (Fig. 4*b*).

3.3 NaCl-0.1 MOLE-% NaBr. — The typical dislocation arrangement found in foils parallel to the primary glide plane is shown in figure 5. It consists nearly exclusively of primary dislocations. The edge dis-

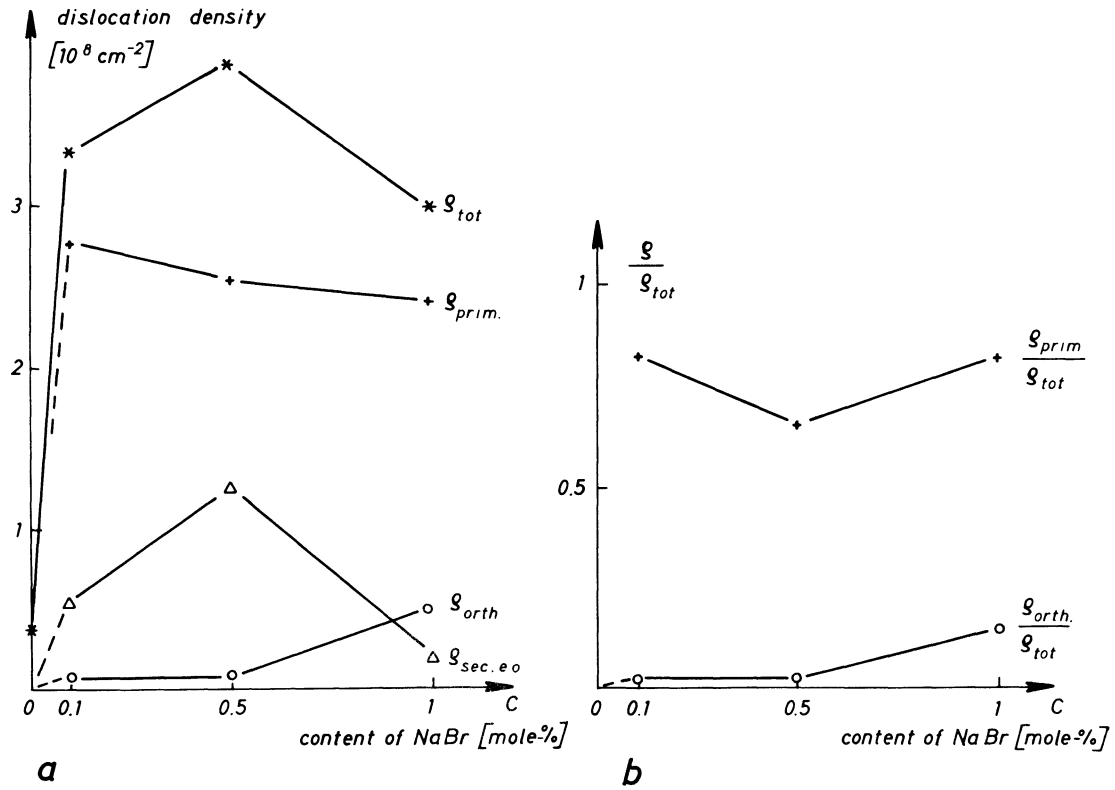


FIG. 3. — *a*) Dislocation densities $\rho$ as a function of NaBr content for a strain $\varepsilon = 6.9$ %. The total dislocation density $\rho_{tot}$ of the pure crystal is extrapolated, $\rho_{prim}$, $\rho_{orth}$, $\rho_{sec\ e.o.}$ denote the primary, the orthogonal and the secondary (excluding the orthogonal) dislocation densities. *b*) Primary or orthogonal dislocation density as fraction of the total dislocation density.

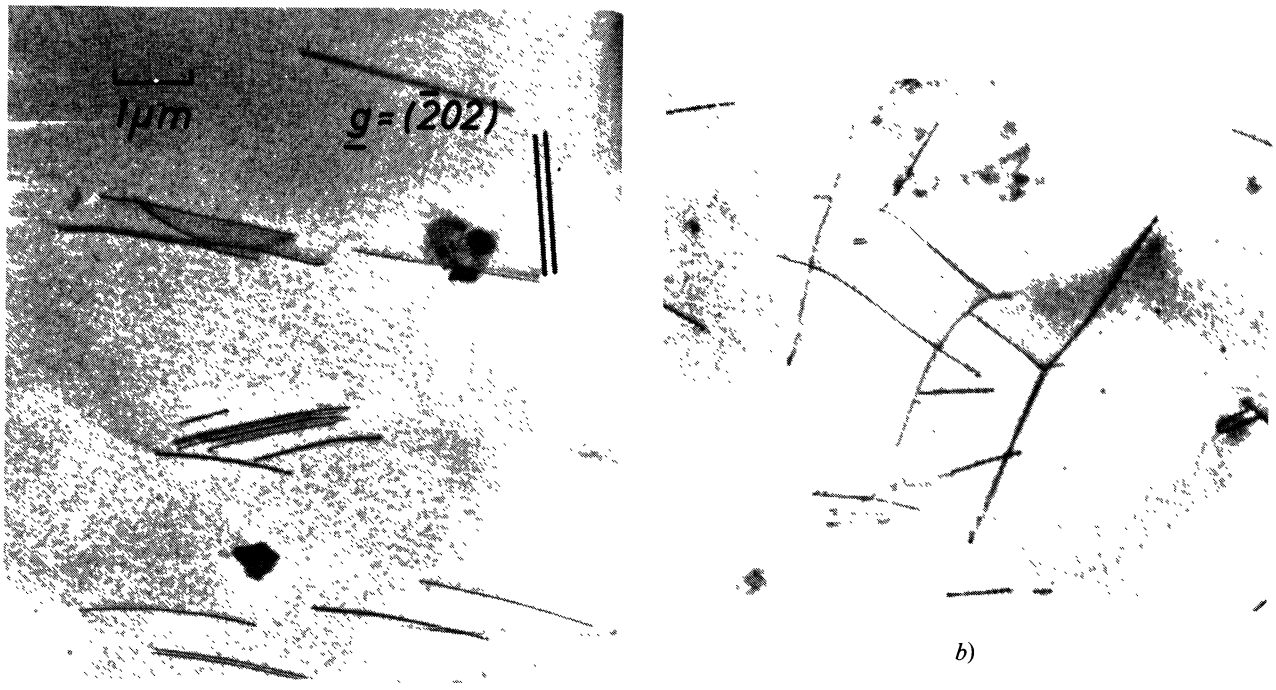


a) b)

FIG. 4. — *a*), *b*) Pure NaCl, resolved strain $\varepsilon = 3\ \%$. Foil inclined 35° to the primary glide plane ({ 111 }-section). The primary Burgers vector is parallel to the diffraction vector **g** (marked by a doubled line, also in the following micrographs). *a* : Region with essentially primary edge dislocation dipoles. *b* : Region with dislocations with screw component.

FIG. 5. — NaCl-0.1 mole-% NaBr. Primary glide plane, primary Burgers vector parallel to g. High density of primary edge dislocation dipoles (*debris*). Primary screw dislocations are anchored at jogs. Encircled : prominant example of an edge dislocation dipole dragged by a screw dislocation, partly pinched-off.

locations are concentrated in more or less dense multipole arrangements (*dislocation braids*). A large number of narrow fragmented edge dislocations dipoles (*debris*) is observed within the braids and in the regions in between. The narrow dipoles and the debris visible in figure 5 correspond to about two third of the total dislocation density.

The screw dislocations are observed to contain many jogs, at which they are pinned as may be deduced from the cusp-like distortions along the dislocation lines. Sometimes the jogs are long enough to be resolved on the micrographs. Frequently narrow dislocation dipoles are trailed along at these sites; a prominent example is encircled in figure 5, part of this dipole is evidently pinched-off from the dislocation to form an isolated edge dislocation loop.

Apart from the fluctuations in the distribution as seen in figure 5, the dislocations are arranged relatively homogeneously on a larger scale. This holds especially also for the distribution in the direction perpendicular to the primary glide plane; no indication of localization into glide band has been found.

In regions with some secondary dislocations in addition to the primary ones, essentially the same type of arrangement as described before is observed. Apart from the few orthogonal dislocations, these secondary dislocations are rather jogged and are located in the dislocation braids indicating strong local interactions with primary dislocations. This feature is common for dislocation braids in pure NaCl [3] and in the higher doped NaCl-NaBr crystals.

3.4 NaCl-0.5 MOLE-% NaBr. — An example of the characteristic dislocation arrangement as observed in thin foils parallel to the primary glide plane is shown in figure 6. The striking feature is that — in contrast to the preceding results (e.g. Fig. 5) — dislocations of screw or nearly screw character are bowed very smoothly, i.e. these dislocations do not, in general, contain any jog, at which they are distorted cusp-like or trail along edge dislocation dipoles. Also in these regions the density of debris is significantly lower than in the NaCl-0.1 mole-% NaBr crystal (compare Fig. 6 and 5).

The arrangement of the edge dislocations is not

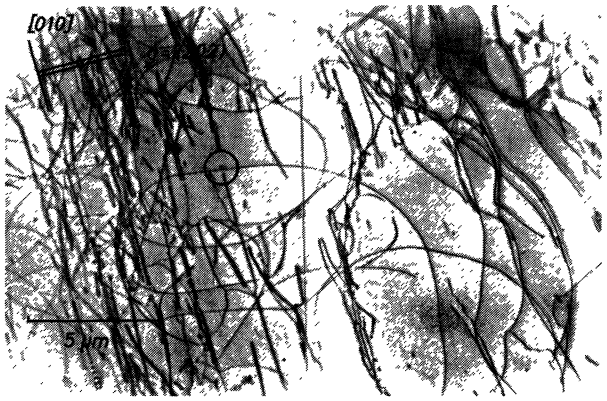


FIG. 6. — NaCl-0.5 mole-% NaBr. Primary glide plane, primary Burgers vector parallel to **g**. Trace of the orthogonal glide plane along [010]. Arrangement of essentially primary dislocations. Circle : Elastic interaction of a primary screw dislocation with an orthogonal dislocation being inclined in the foil. Orthogonal dislocations can be distinguished from primary ones by their symmetric residual contrast occurring for $\mathbf{g}.\mathbf{b} = 0$ (**b** : Burgers vector) [16].

significantly different from that of the less doped crystal (section 3.3). The edge dislocations occur on the whole in multipoles, that also contain a considerable fraction of fragmentary edge dislocation dipoles and some secondary dislocations. Again, the dislocations are distributed relatively homogeneously in and also perpendicular to the primary glide plane.

Some orthogonal dislocations are visible in figure 6. Their arrangement and their interaction with the primary dislocations may be investigated relatively easily in foils cut parallel to the orthogonal glide plane. Generally (Fig. 7) isolated orthogonal dislocations with dominant screw character, containing several jogs are observed. An increased density of primary dislocations is always found along the line of these dislocations. These primary dislocations have partly screw character, as may be deduced from the short contrast segments projected on the trace of the primary glide plane. Closer inspection of the two mutually interacting dislocations in the encircled area in figure 6 leads to the same result.

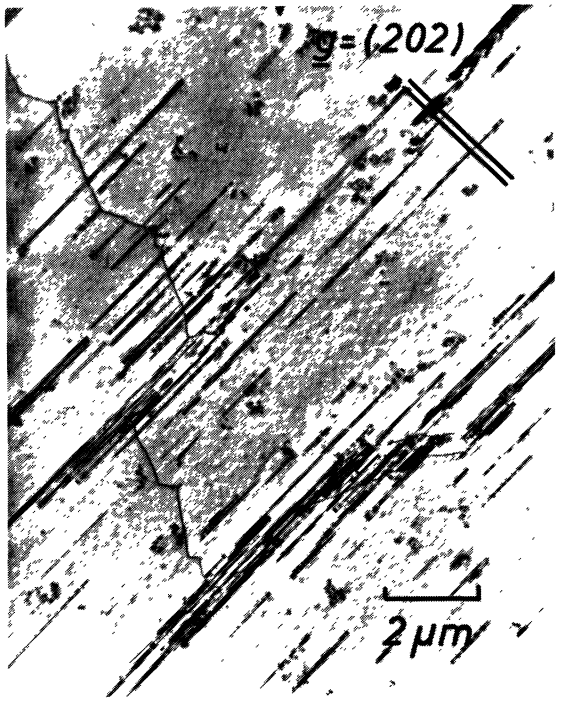


FIG. 7. — NaCl-0.5 mole-% NaBr. Foil parallel to the orthogonal glide plane. One orthogonal dislocation in screw orientation interacting with a large number of primary dislocations (imaged in residual contrast).

3.5 NaCl-1 MOLE-% NaBr. — Regions containing essentially primary dislocations, arranged as described in section 3.4 (e.g. Fig. 6) are found. In addition, arrangements containing a considerable fraction of orthogonal dislocations are observed relatively frequently. These will be considered with the aid of figure 8 showing a section parallel to the primary glide plane. The orthogonal dislocations are distinguished by their symmetric, sometimes double-lined contrast (residual contrast [16]). In the upper part of figure 8, e.g. at E, a large number of orthogonal dislocations with essentially edge character are seen lying along the trace of their glide plane. Orthogonal dislocations


FIG. 8. — NaCl-1 mole-% NaBr. Primary glide plane. Trace of the orthogonal glide plane approximately horizontal. Arrangement of primary dislocations interacting with orthogonal ones, which have at E nearly edge, at S nearly screw character. Arrows indicate polygonization arrangements (walls) of primary edge dislocations ; the contrast change at the wall at top is due to the lattice rotation caused by such walls.

lying obliquely in the foil, thus having a screw component give rise to short, frequently modulated contrasts (e.g. at S). They are found in the whole region of figure 8.

Figure 8 indicates also a relatively homogeneous distribution of the dislocations in the primary glide plane. This is also found in foils perpendicular to the primary glide plane. In addition, the primary edge dislocations tend strongly to arrange themselves in polygonized form. Two examples are indicated by arrows in figure 8. As a particular feature of such polygonization walls, shown in figure 9 at K, the edge dislocations frequently deviate kink-like as a whole (e.g. also [17]). Each of these deviations is caused by only one orthogonal dislocation with partly screw character, which acts obviously as a strong barrier to the primary edge dislocations.

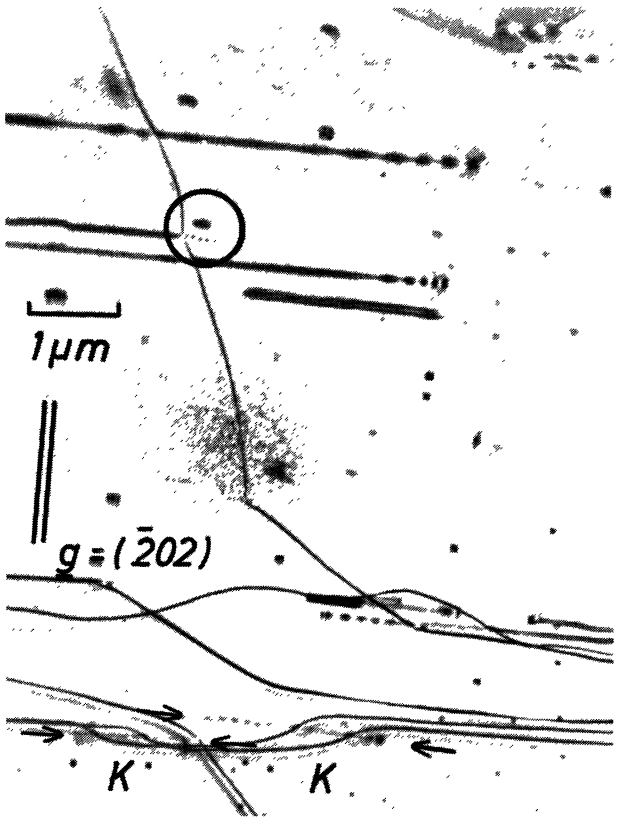


FIG. 9. — Enlarged section of figure 8. Circle : mutual interaction of a primary and an orthogonal screw dislocation. At bottom section through a polygonization wall ; the primary edge dislocations possess the same sign of the Burgers vector as indicated by the satellite contrasts lying each at the same side of the strong dislocation images. Arrows indicate two orthogonal dislocations each causing a deviation in the polygonization wall.

Due to their large number, polygonization walls are likely to be found in foils perpendicular to the primary glide vector. A section of such a wall is shown in figure 10. The primary edge dislocations, imaged in residual contrast, indicate a remarkably equidistant polygonization arrangement. Orthogonal dislocations sometimes align along the primary edge dislocations

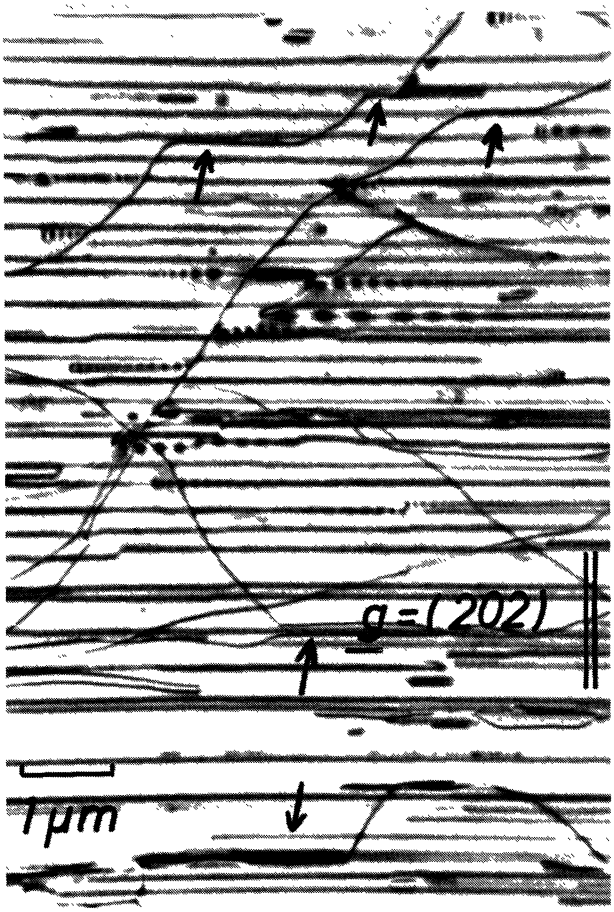


FIG. 10. — NaCl-1 mole-% NaBr. Orthogonal glide plane. Trace of the primary glide plane horizontal. Section through a polygonization wall. Nearly equidistant primary edge dislocations (see in residual contrast) and a few orthogonal dislocations.

(arrows), obviously due to an elastic short-range interaction. The contrast experiments possible so far cannot decide whether or not recombinations occur between these dislocations leading to the formation of $\langle 100 \rangle$-dislocations.

4. **Discussion.** — 4.1 PRELIMINARY REMARK. — In solid solution hardened crystals a considerable friction stress acts on the dislocations. Therefore, during unloading the deformed crystals each dislocation relaxes only until a balance between backdriving stresses (resulting from the line tension and also from the internal stress field due to the surrounding dislocations) and the friction stress is achieved. In our case of the weakly deformed alloy crystals the friction stress is comparable to the flow stress increment $\Delta\tau$ caused by work hardening (e.g. Fig. 2). Accordingly only minor or no relaxation is expected, leaving many features typical for the stress-applied state to be observed. One of these is the abundant occurrence of screw dislocations (e.g. Fig. 5), which otherwise can annihilate to a large extent during or after unloading the crystals by cross-slip. The frequent absence of screw dislocations has occasionally given rise to misinterpretations (e.g. [18]).

In the following the results shall be discussed with reference to the deformation mechanisms in stage I of pure NaCl. This extrapolation from the alloys remains necessarily qualitative in nature. A more quantitative interpretation requires knowledge on the glide of dislocations in these alloys, which is not available so far (obtainable by e.g. etch pit and slip line investigations, by determination of parameters of thermal activation and of flow stresses in other than { 110 }-planes). In section 4.3 some observations made in the stronger doped crystals, but thought to be of importance also for pure NaCl, are considered.

4.2 DEFORMATION MECHANISMS IN STAGE I OF PURE AND OF NaCl-0.1 MOLE-NaBr CRYSTALS. — Two strikking features are observed in NaCl-0.1 mole-% NaBr crystals : a high density of primary edge dislocation loops and a large number of primary screw dislocations dragging behind them dipoles at jogs. A similar arrangement is present also in pure NaCl (section 3.2). It is strongly suggested by these observations that during deformation the screw dislocations have to bow between jogs thereby dragging edge dislocation dipoles behind them, which may eventually pinch off. Jogs with heights ranging from one to several thousand interionic distances can be created continuously by cross-slip of the screw dislocations which is easy in NaCl [5, 19], and by incorporation of edge dislocations dipoles during glide.

Such a drag mechanism has been discussed in detail by Johnston and Gilman (e.g. [20]). Its operation in NaCl was indicated by etch pit investigations [21] and in particular by measurements of the volume density [22]. After deformation a large volume expansion was found in NaCl, which could only be explained by a high density of atomic defects [22]. (An explanation on the basis of the introduced dislocation density failed by a factor of 100). The drag mechanism is consistent with this conclusion, since the edge dislocation dipoles may be decomposed by several processes into atomic defects either in clustered or isolated form. Frequently dipoles are observed to be broken into rows of small loops, probably due to pipe diffusion [3, 17]. In addition, dipoles may be destroyed by glide dislocations cutting them, and dipoles having a width of one or two interionic distances may dissociate on energetic grounds into an atomic defect cloud (e.g. [23]).

Two estimates using TEM results lend support to the drag mechanism. The critical diameter of a Frank-Read source is given approximately by :

$$D = \frac{Gb}{\tau} \qquad (1)$$

$G$ : shear modulus (= 18.5 GN/m$^2$), $b$ : modulus of the Burgers vector, (= 0.4 nm), $\tau$ : shear stress acting on the dislocation. With $\tau \sim 1$ MN/m$^2$ (excluding the friction stress) we obtain $d \sim 7$ μm, which is the right order of magnitude (e.g. Fig. 5). This is in accordance with an estimate of the dipole widths observed in pure NaCl (Fig. 4*a*). If the dipoles were created by mutual trapping of gliding edge dislocations, one would expect widths up to the passing distance $d$. This distance may be written :

$$d = \frac{G.b}{4\,\pi(1 - \nu).\tau} \qquad (2)$$

$\nu$ : Poisson's ratio (= 0.25). With the flow stress of the pure NaCl crystal of $\tau = 0.7$ MN/m$^2$ (e.g. Fig. 2) : $d \approx 1$ μm. This is much larger than the observed widths of $\lesssim 0.1$ μm. Thus the dipoles are very probably left behind by gliding screw dislocation ; the small widths can be attributed to the expected high frequency of relatively small jogs in screw dislocations.

Stress-relaxation experiments show [24, 25] that a relatively small thermally activated stress component contributes to the flow stress of pure NaCl at room temperature. It increases during deformation from zero onwards, indicating a deformation-induced origin. The present results suggest two different types of mechanisms which may in principle account for this component. Firstly, an elastic interaction of the glide dislocations with the generated atomic defects and their agglomerates has to be visualized, which may be overcome by thermal activation [23]. Secondly in edge dislocations jogs are always found, which, of course, can glide conservatively along with their edge dislocations. At room temperature, however, glide on the planes of the jogs ({ 100 }, { 111 } and higher indices planes [19]) requires thermal activation [5]. A corresponding drag may be exerted on the gliding edge dislocation segments attached to the jog (e.g. [26]). Further experiments are necessary to decide which of the two mechanisms is predominant in NaCl.

4.3 DISLOCATION ARRANGEMENT IN THE HIGHER DOPED CRYSTALS. — Two features shall be considered : the general absence of jogs in screw dislocations and the interaction of primary with orthogonal dislocations.

Two reasons for the absence of jogs in screw dislocations may be found. The straightforward one is that cross-slip and thus the formation of jogs is largely suppressed by the $Br^-$-content. This, however, is unlikely, since in this case strongly localized glide bands should occur ; in contrast, a quasi-homogeneous distribution of dislocations perpendicular to the primary glide plane has been observed. If, however, jogs are continuously created during deformation, an effective process should exist to eliminate them from screw dislocations. Elimination could be performed by glide along the line of the screw dislocation. This may occur under the action of the resultant stress exerted on the jog by the attached bowed screw dislocation segments and in addition by an applied stress. In pure crystals, this glide is obviously hindered (section 4.2), very probably because the stress to move a jog in its glide plane is several times that to move the screw dislocation in its { 110 }-plane [5]. It seems reasonable

that at a certain alloy-induced friction the intrinsic differences in the glide properties of jogs and attached screw dislocations are less important. The ratio of the mobility of screw dislocations to that of the jogs may therefore be reduced so that a jog may glide sidewards before the attached screw segments have bowed to the critical radius. Fcc metals, for example, represent extremes in this respect, since there dislocation and jogs (apart from some with one atomic distance height [27]) have equivalent glide planes (of { 111 }-type). In consequence of this explanation, the dragging of edge dislocation dipoles should be suppressed in pure NaCl at very low strain rates, if the screw dislocations move slowly and if time enough is provided for the jogs to glide sidewards. At high temperatures the glide of the jogs is facilitated, which may result also in a suppression of the dragging mechanism. Especially in the latter case non-conservative processes could interfere.

The TEM observations indicate that dislocations of the orthogonal glide system represent strong short-range obstacles for primary dislocations (e.g. Fig. 7). Frequently screw or nearly screw dislocations of both systems are observed to bow around each other (e.g. Fig. 9). Such an interaction process has been anticipated in the work-hardening theory of alkali halides developed by Frank for the case of symmetrical double glide [23, 28]. Glide polygonization of primary edge dislocations is obviously aided and stabilized by the orthogonal screw and edge dislocations (e.g. Fig. 10). According to investigations by etch pits [22] and X-ray topography [4] of pure NaCl, glide polygonization walls nucleate at orthogonal glide zones.

It is known from [001]-orientated crystals that the single glide of pure NaCl develops after a short period ($< 1\ \%$ strain) of activation of all the glide systems with the same maximum Schmid factor [15, 22]. Fluctuations in the local dislocation distribution, leading in one particular glide system to a local dislocation density above the average, may cause latent hardening of the competing systems with subsequent suppression of their activity. For oblique glide systems latent hardening has been measured (e.g. [29]). Our observations on the behaviour of orthogonal dislocations suggest also an appreciable latent hardening for orthogonal glide systems, which could account for the observed single glide in orientations for double glide (L. Kemter, A. Strecker, H. Strunk, unpublished). This should be clarified in the future by specifically designed experiments.

5. **Conclusions.** — [001]-orientated crystals deform essentially by single slip, although four equivalently stressed glide systems of type $\{ 110 \} \langle \bar{1}10 \rangle$ are present. In this glide geometry dislocations with mutually perpendicular Burgers vectors obstruct each other, acting as strong short-range obstacles. This may be partly responsible for the development of single slip, since the multiplication of dislocations of one kind, occurring incidentally in lower densities, can be suppressed.

The TEM observations in pure and weakly alloyed NaCl crystals can be interpreted in terms of the debris mechanism proposed by Johnston and Gilman. Accordingly the stage I deformation of pure NaCl crystals is determined by the bowing of primary screw dislocations between jogs and the dragging of edge dislocation dipoles at such jogs.

At higher NaBr contents, this mechanism is suppressed, probably because intrinsic differences in the glide properties on different planes become less important in the presence of a strong solid solution hardening.

**Acknowledgments.** — The author benefited by discussions with Dr. M. Wilkens. Dr. H. Mughrabi critically read the manuscript.

## References

[1] STRUNK, H., *Phys. Stat. Sol.* (a) **11** (1972) K 105.
[2] STRUNK, H., Proc. III Int. Conf. High Voltage Electron Microscopy, P. R. Swann, C. J. Humphreys and M. J. Goringe eds. (Academic Press, London/New York) 1974, p. 285.
[3] STRUNK, H., *Mater. Sci. Eng.* **27** (1977) 225.
[4] STRUNK, H., *Mater. Sci. Eng.* **26** (1976) 231.
[5] HAASEN, P., *J. Physique Colloq.* **34** (1973) C9-205.
[6] HESSE, J., *Phys. Stat. Sol.* **21** (1967) 495.
[7] POOLEY, D., *Proc. Phys. Soc.* **87** (1966) 245.
[8] HOBBS, L. W., Proc. IV. Europ. Regional Conf. on Electron Microscopy, D. S. Bocciarelli ed., Tipografia Poliglotta Vaticana, Vol. **1** (1968) 265.
[9] HOBBS, L. W., *J. Physique Colloq.* **34** (1973) C9-227.
[10] FINEMAN, M. A. and WALLACE, W. E., *J. Am. Chem. Soc.* **70** (1948) 4165.
[11] LABUSCH, R., *Acta metall.* **20** (1972) 917.
[12] OKUDA, S., WATANABE, J., YAMADA, T. and SOEJIMA, S., *Japan J. appl. Phys.* **7** (1968) 1422.
[13] WIMMER, F. T., KOBES, W. and FINE, M. E., *J. appl. Phys.* **34** (1963) 1775.
[14] HESSE, J., *Phys. Stat. Sol.* **9** (1965) 209.
[15] KEMTER, L. and STRUNK, H., *Phys. Stat. Sol.* (a) **40** (1977).
[16] HIRSCH, P. B., HOWIE, A., NICHOLSON, R. B., PASHLEY, D. W. and WHELAN, M. J., *Electron Microscopy of Thin Crystals*, Butterworths, London/Washington 1965.
[17] STRUNK, H., Proc. IV. Internat. Conf. on High Voltage Electron Microscopy, B. Jouffrey and P. Favard eds (Société Française de Microscopie Electronique, Paris) 1976, p. 229.
[18] MUGHRABI, H., *Phil. Mag.* **18** (1968) 1211.
[19] STRUNK, H., *Phys. Stat. Sol.* (a) **28** (1975) 119.
[20] GILMAN, J. J. and JOHNSTON, W. G., *J. appl. Phys.* **31** (1960) 632.
[21] DAVIDGE, R. W. and WHITWORTH, R. W., *Phil. Mag.* **6** (1961) 217.
[22] DAVIDGE, R. W. and PRATT, P. L., *Phys. Stat. Sol.* **6** (1964) 759.
[23] FRANK, W., *Mater. Sci. Eng.* **6** (1970) 121.
[24] GUPTA, I. and LI, J. C. M., *Mater. Sci. Eng.* **6** (1970) 20.
[25] SPRACKLING, M. T., *Phil. Mag.* **27** (1973) 265.
[26] STRUNK, H. and FRYDMAN, R., *Mater. Sci. Eng.* **18** (1975) 143.
[27] SEEGER, A., *Phil. Mag.* **46** (1955) 1194.
[28] FRANK, W., *Mater. Sci. Eng.* **6** (1970) 132.
[29] NAKADA, Y. and KEH, A. S., *Phys. Stat. Sol.* **32** (1969) 715.